Journal of Petroleum & Environmental Biotechnology

OPEN ACCESS Freely available online

Research Article

A Field Development Plan for Catshill Brown Oilfield in Trinidad Utilizing Waterflood Simulation

Paul Amihere-Ackah[1]*, Prof. Raffie Hosein[1] and Benjamin Makimilua Tiimub[2]

[1]University of the West Indies, St Augustine Campus, Trinidad and Tobago; [2]College of Environmental and Resource Sciences, 310058, Zhejiang University, Hangzhou, P.R. China

ABSTRACT

The identification of new oil fields onshore Trinidad and Tobago has become almost impossible. Therefore the possibility of producing by-passed hydrocarbon accumulation from the matured Catshill field was determined through a holistic field development plan using waterflooding. The field development plan involved detailed reservoir characterization study. There were two phases of development plans considered.

(1) Injecting water above the bubble point for a new field development

(2) Injecting water below the bubble point using existing field data. Effective use of petrel aided the building of all geological maps of the area.

Maps generated in Petrel were exported to Computer Modelling Group (CMG) for detailed reservoir simulation study. The estimated oil in place was 27.541 MMSTB. Primary production yielded 27.2% recovery factor which was less than half of the oil in place. Implementation of water injection above the bubble point pressure yielded 49.8% recovery factor when produced for 10 years. By injecting water below the bubble point pressure using staggered line drive pattern, the recovery factor was 39.4%. It can be concluded that developing a field using waterflooding is best when pressure is high. However, there could still be significant recovery (39.4%) when field is matured. Economically, production will not be profitable if the oil price goes below 46 US$/bbl.

Keywords: Field development; Reservoir; Matured oilfield; Waterflood simulation; Catshill

INTRODUCTION

Oil field development is a multi-disciplinary approach that comprise of parameters relating to geological and structural characteristics, reservoir characteristics through to operational scheduling and economic analysis and evaluation [1]. Reservoir lifecycle starts at exploration and discovery [2]. When discovered it is produced until it ends at abandonment 2010. Many discovered field are ever diminishing and matured [3]. Increasing water and gas production, decreasing pressure, and aging equipment are indicators of field maturity [4]. Trinidad discovered oil in 1876 but commercial production only began in 1908 [5]. Trinidad and Tobago has record in petroleum sector for more than one hundred (100) years with cumulative production of more than three (3) billion barrels of oil. According to Ernst and Young [6] proven crude oil reserves as at 2013 were estimated at 728 million barrels a publication by the Energy Information Administration (EIA). This indicates that the possibility of fields becoming matured is high. A holistic development scheme for recovering oil from these matured fields is much necessary. Among such fields in Trinidad is the Catshill oil field.

According to the Ministry of Energy and Energy Industries in 2009 [7], the first well drilled in Catshill was in November 1950. The Catshill field is divided into two main parts, the Northeast and Southeast, each part of the field was discovered by the drilling of CO-3 and CO-5 wells respectively in 1952. The two subdivision of the field is marked by a major fault known as the Boomerang fault which has a marked difference on either side with respect to biofacies and lithofacies. This research evaluates the Southwest of the Catshill Field. The Southwest of the field produces from the k-sand commonly known as the CO-30 sand. Most of the oil production comes from the sands that are of Upper Miocene age [8]. The field has been in production for more than 40 years with a decrease in pressure and production making the reservoir

Correspondence to: Paul Amihere-Ackah, 1Department of Chemical Engineering, Faculty of Engineering, University of the West Indies, St Augustine Campus, Trinidad and Tobago, Tel: +233549512469; E-mail: amihereackahpaul112@gmail.com

Received: April 13, 2020, **Accepted:** May 04, 2020, **Published:** May 11, 2020

Citation: Amihere-Ackah P, Tiimub BM (2020) A Field Development Plan for Catshill Brown Oilfield in Trinidad Utilizing Waterflood Simulation 11:405. doi: 10.35248/2157-7463.20.11.405

undersaturated [9]. The decline in oil production due to matured field is also reported recently by Cambridge Energy Research Associates where they estimated that the weighted decline of production from all existing world oil fields was roughly 4.5% in 2006 CERA [10]. which is in line with the 4-6% range estimated by ExxonMobil [11]. These reports depicts the need for a robust field development plan to determine further oil recovery from the mature field.

Mature fields development which consists mostly of secondary and tertiary production, account for more than 70% of the World's oil and gas production. Averagely the recovery factor being 70% for gas and about 35% for oil [12-14]. With optimized waterflooding and enhanced oil recovery methods, there is potential to increase the amount of petroleum that can be economically produced from matured reservoirs [15]. The development phase fully integrated reservoir characterization. These are theoretically the ideal solutions, since complex 3D models are able to integrate localized geological characteristics and the full physics of simulation [16-18]. In other to achieve this, one needs to know the amount and location of the target oil first [4]. Locating the remaining oil and building a development plan have enormous importance [19,20]. This study approach utilized waterflood simulation.

Reservoir simulation according to various literature including but not limited [21-24] can be employed in well in inverse engineering problems for optimizing existing numerical models and couple the dynamic and historic data (production) in the simulation. Waterflooding can lead to the recovery of about one-third of the original oil in place (OOIP) [25]. This study therefore focused on development of an existing onshore Catshill brown oil field by presenting a comprehensive development plan using waterflood simulation (Figures 1-17 and Tables 1-6). It focused on:

(1) Waterflood simulation above the bubble point for a new field development

(2) Waterflood simulation below the bubble point using existing field data taking into account the recovery factors from each scenario.

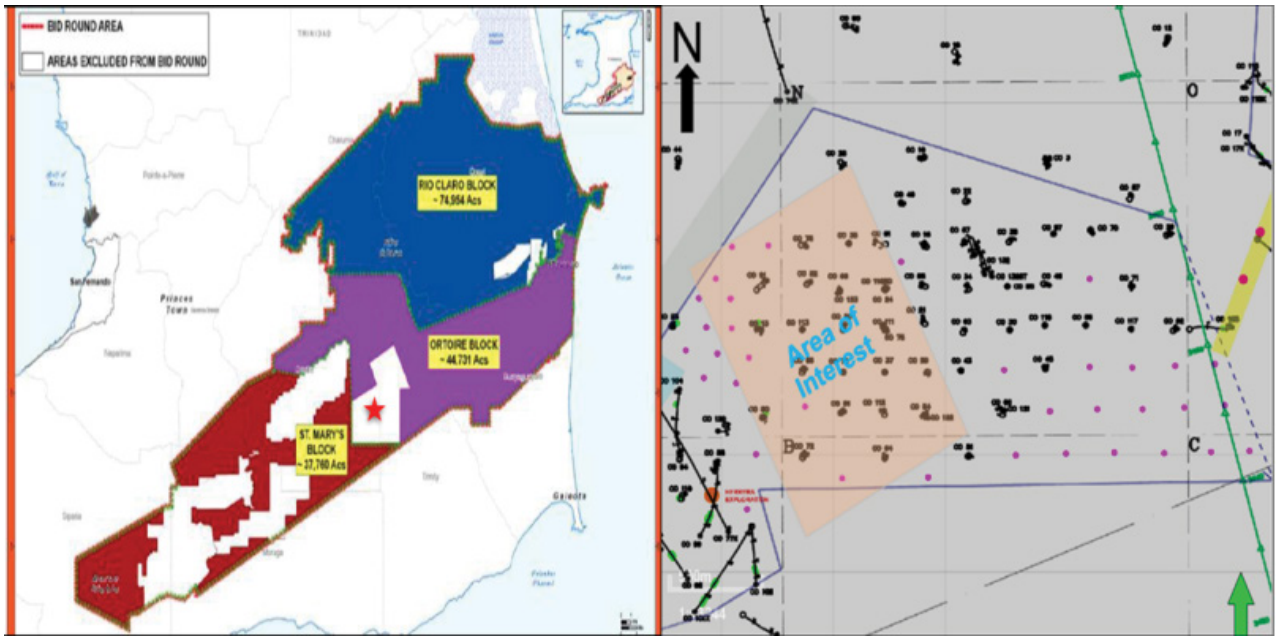

Figure 1: Catshill field within the Ortoire Block South Trinidad (left) and Selected area of study from the base map (right).

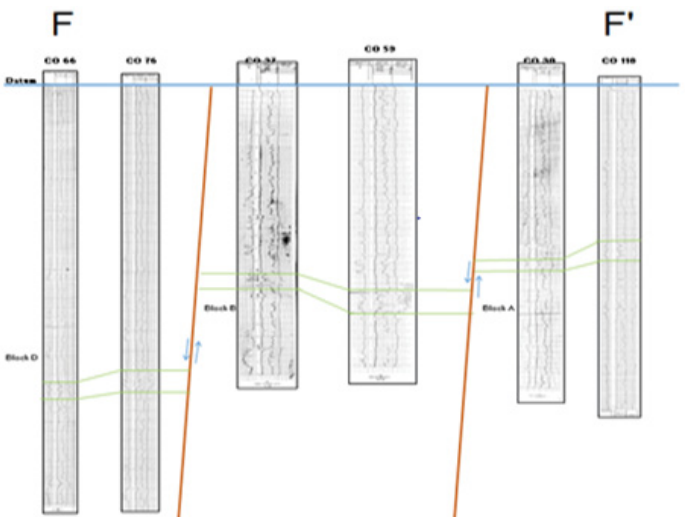

Figure 2: Structural cross section along strike Line F-F'.

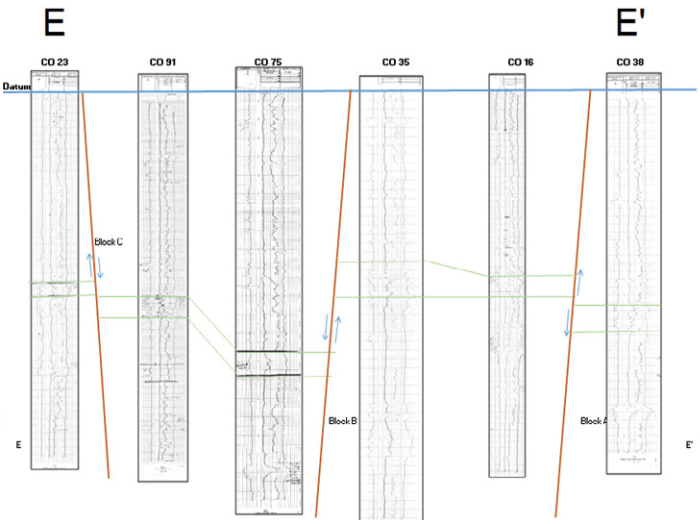

Figure 3: Structural correlations for fault analysis along strike line E-E'.

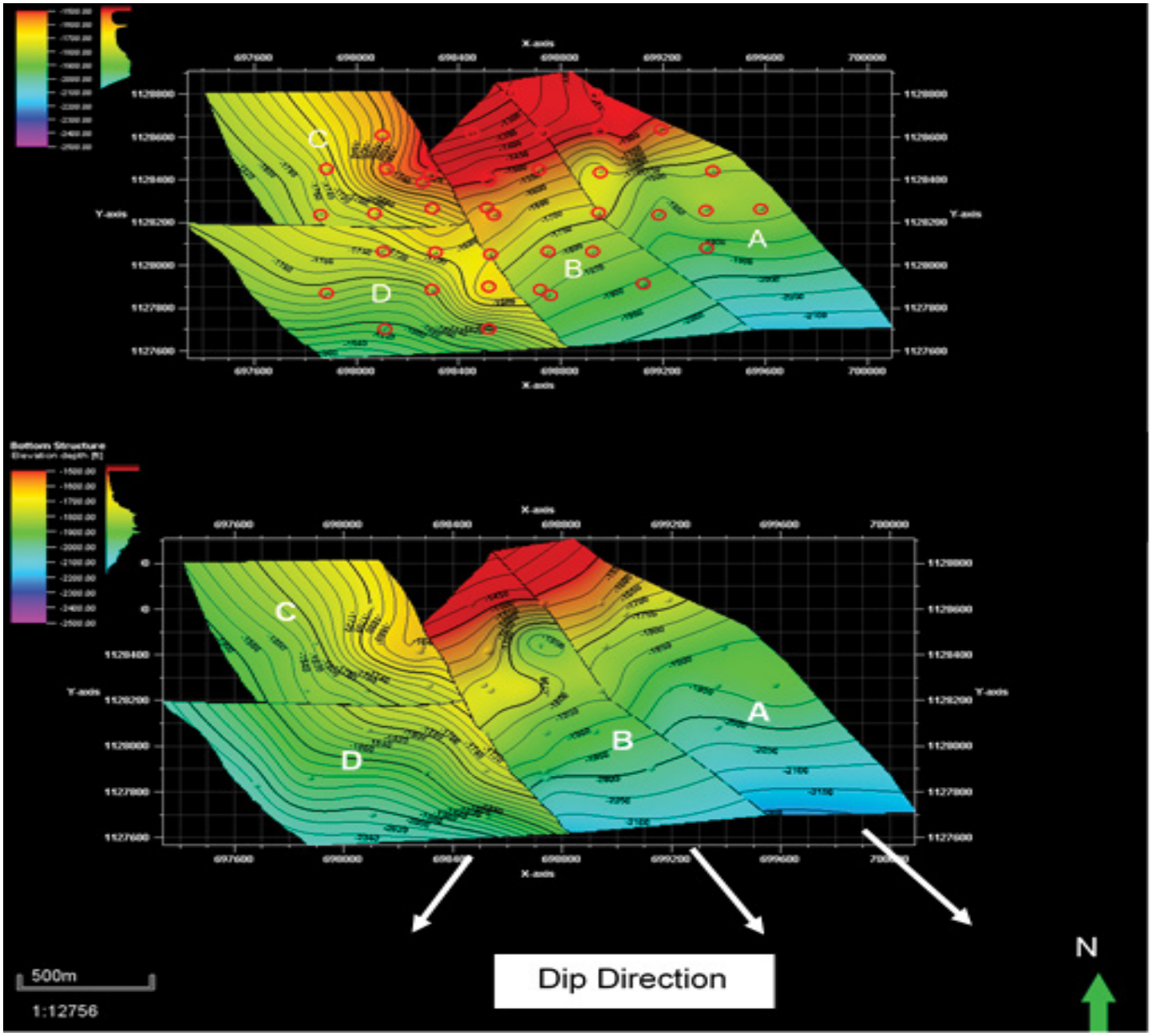

Figure 4: Top and bottom structure map respectively generated from petrel.

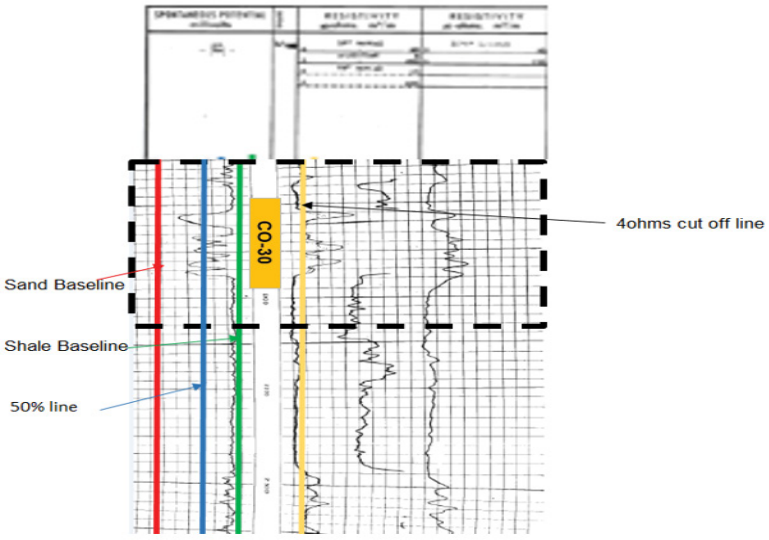

Figure 5: Procedure used to determine the net sand thickness excluding all shale intervals.

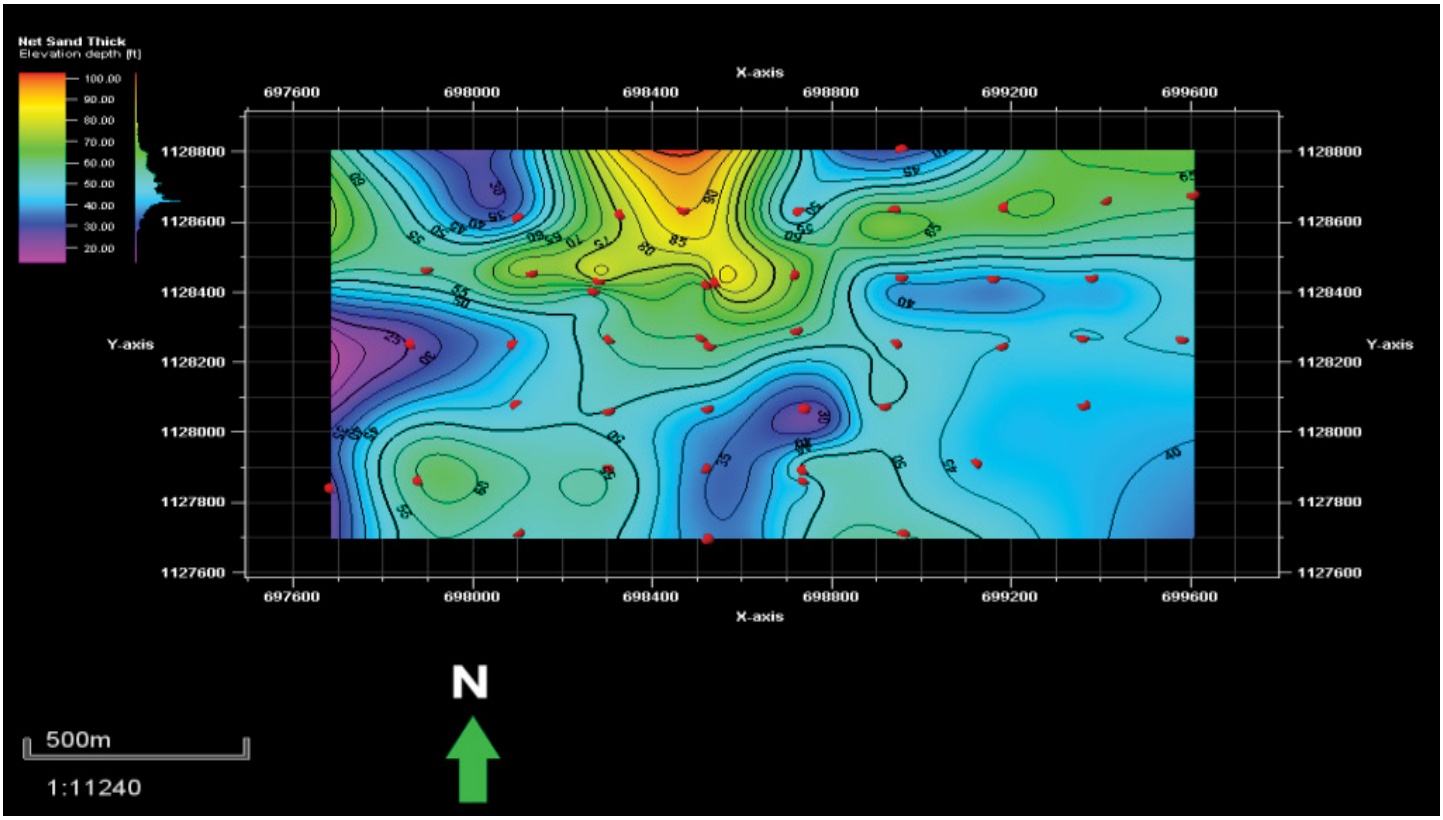

Figure 6: Net sand map of CO-30 sand.

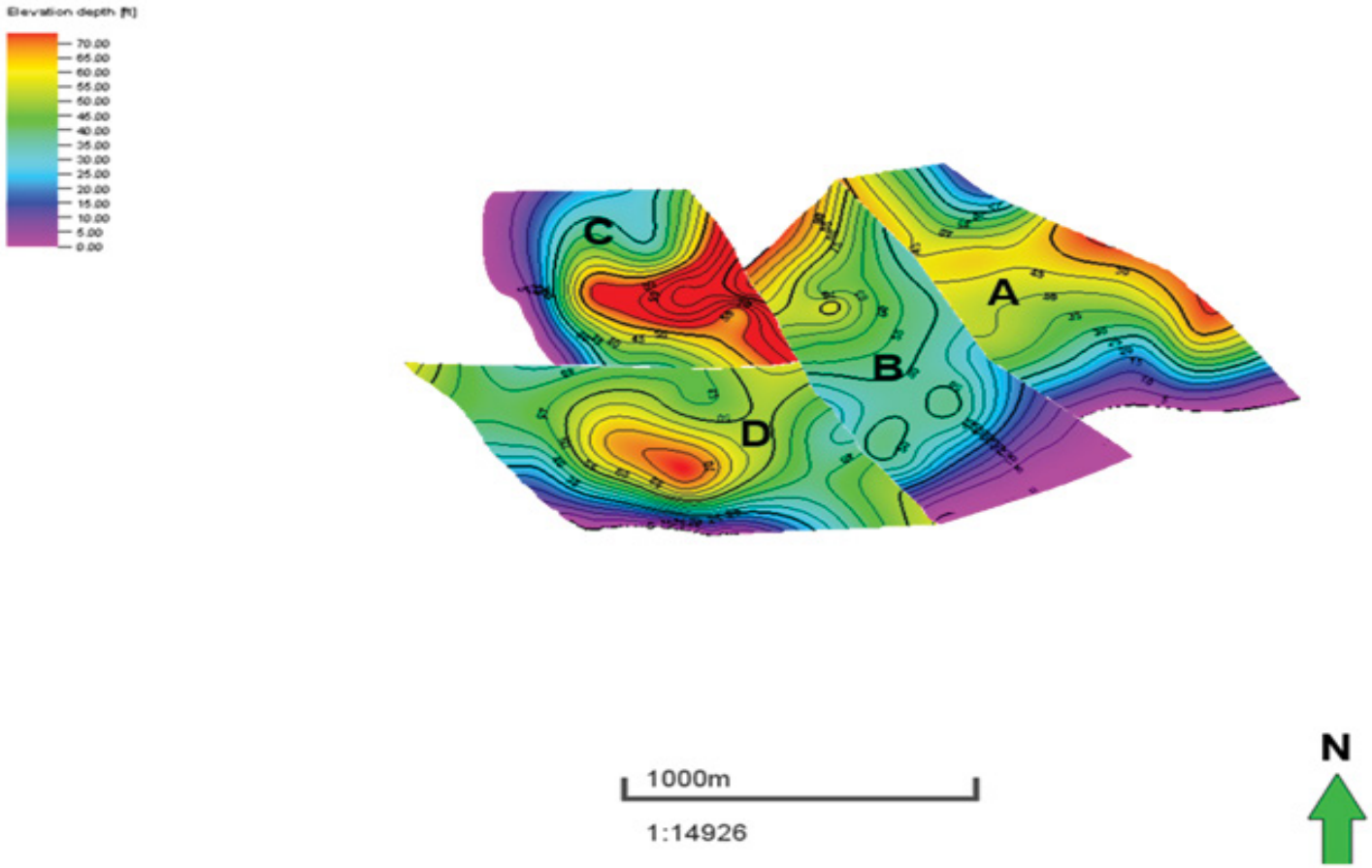

Figure 7: Net oil sand map of the CO-30 sand.

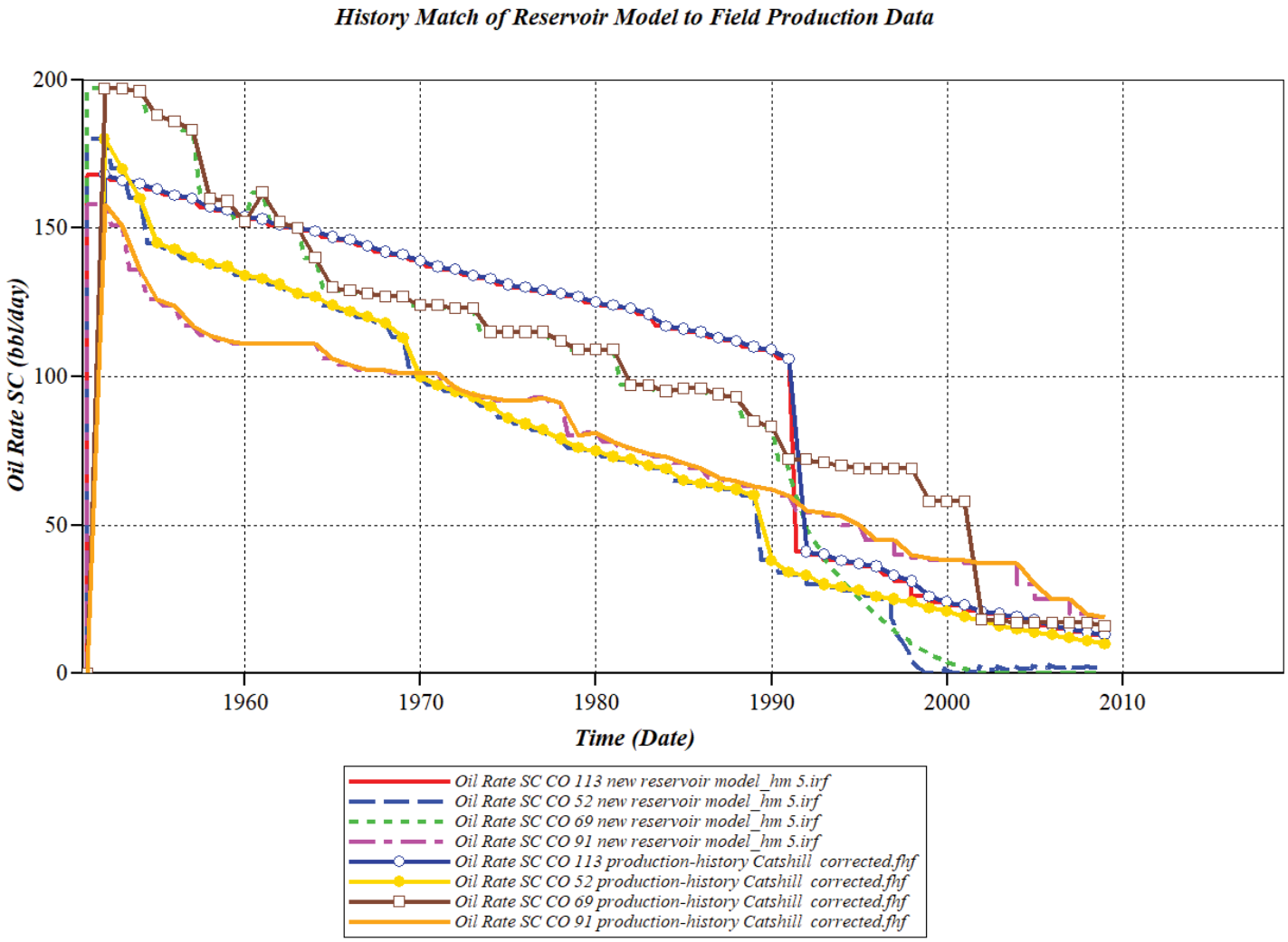

Figure 8: History matching of all wells to the field production data.

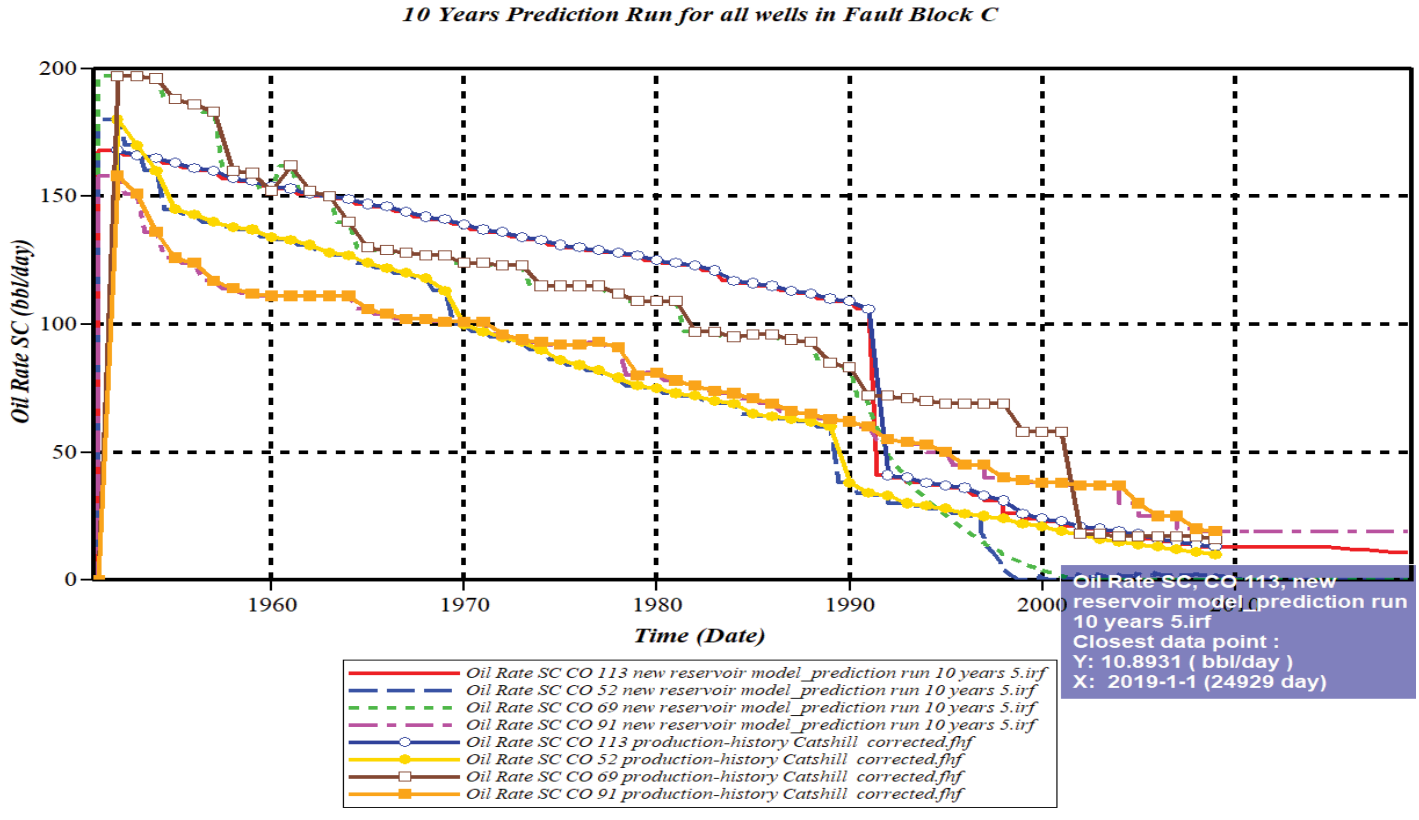

Figure 9: Ten year prediction run for all the wells of fault block C.

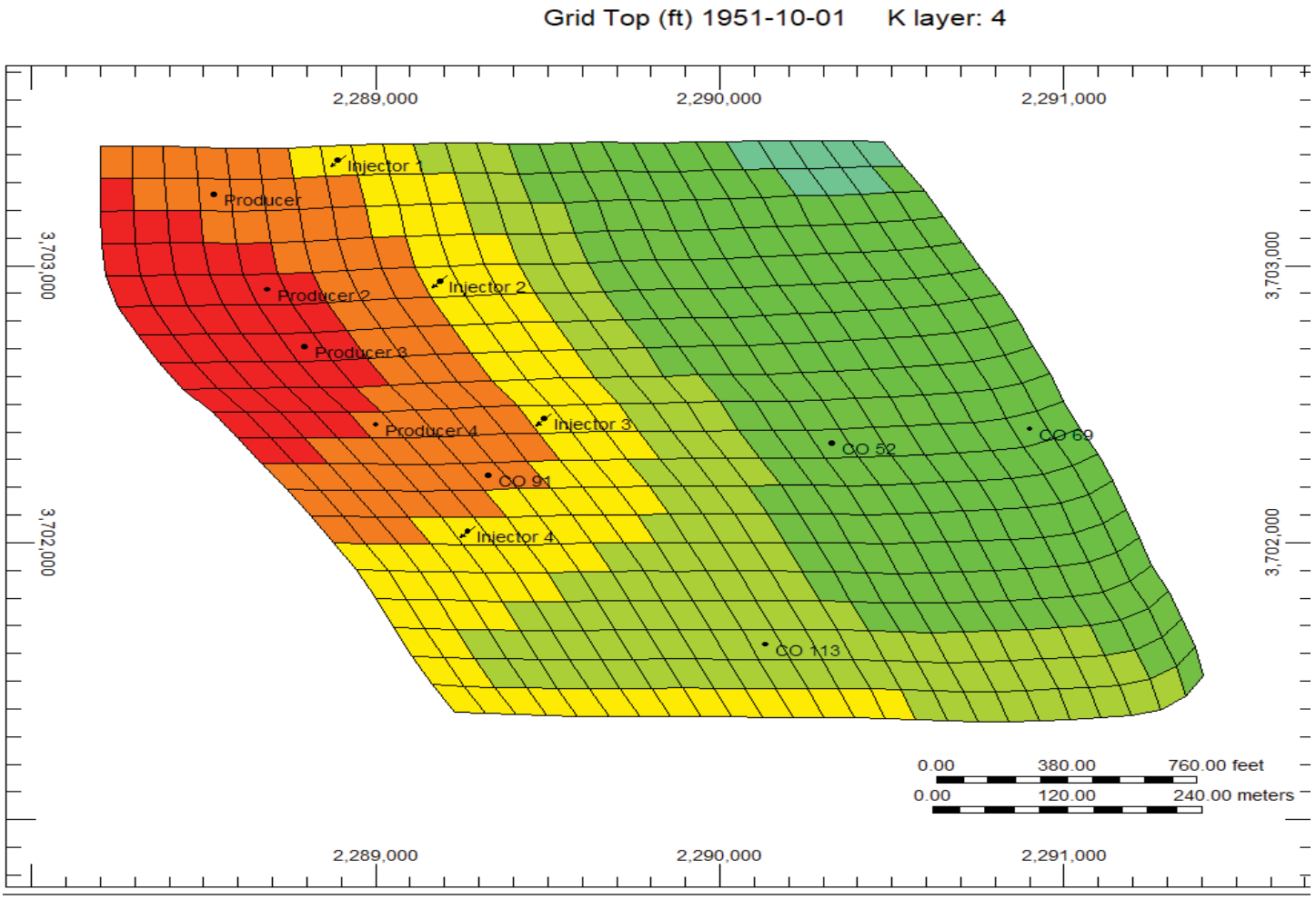

Figure 10: Aerial view of location of injectors and producers for the staggered line drive pattern at start of production.

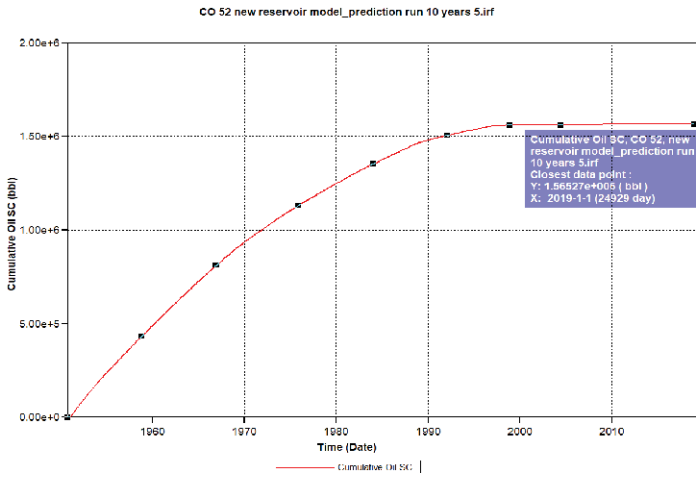

Figure 11: Cumulative oil production for 10 years with no water injection.

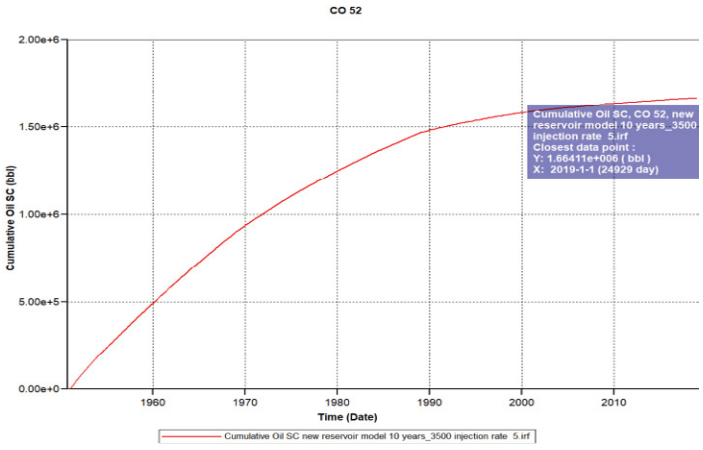

Figure 12: Cumulative oil production for 10 years with water injection at 3500 b/d.

MATERIAL AND METHODS

Geological analysis of the field

The field was intelligently and holistically reviewed using well logs, base maps, well files, seismic lines and field reports. Based on the reviewed data and reports of the field, an area of interest was chosen from the base map for further analysis (Figure 1). The field was mapped to determine faults and possible contacts (Figure 3 and Appendix 1, Table 10 and 13). The regional faulting, initial dip and strike direction were identified using guide from the Kugler map. This followed type log signature identification for the CO-30 sand (Appendix 1, Figure 18) and pulling section lines along dip and strike to develop cross section as well as determining sand continuity from stratigraphic cross section (Appendix 1, Figure 20). From the logs, the Top of Sand (TOS) and Bottom of Sand (BOS) were carefully marked (Appendix 1, Figure 18). The True Vertical Depth Sub Sea (TVDSS) were calculated using the available well files to obtain elevation data for each well (Appendix 1, Table 13). To do the correlation, the SP and Resistivity log signatures present in the CO-30 sand were used to identify sand bodies of similar pattern that would have been deposited at the same time and as a

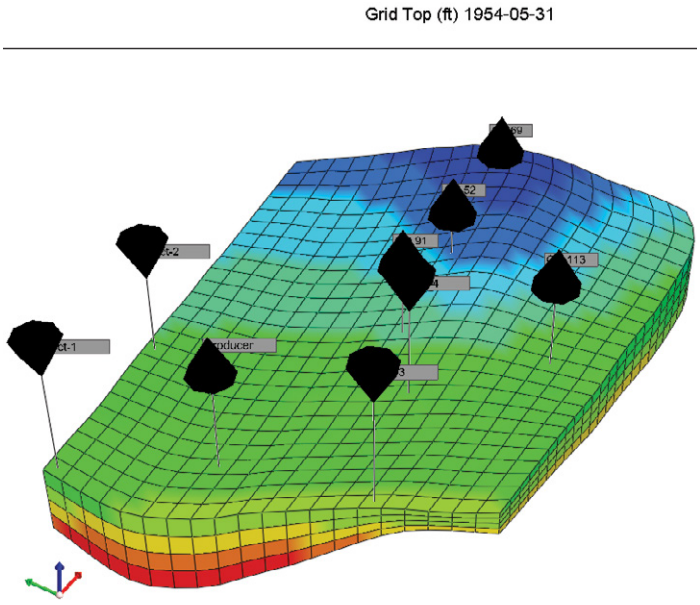

Figure 13: 3D view of the location of the five spot well pattern in CMG.

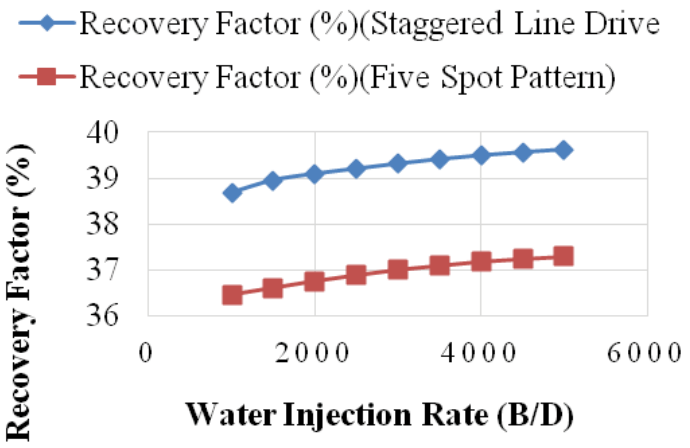

Figure 14: Graphical presentation of the recovery factors from both flood patterns from 2009-2019.

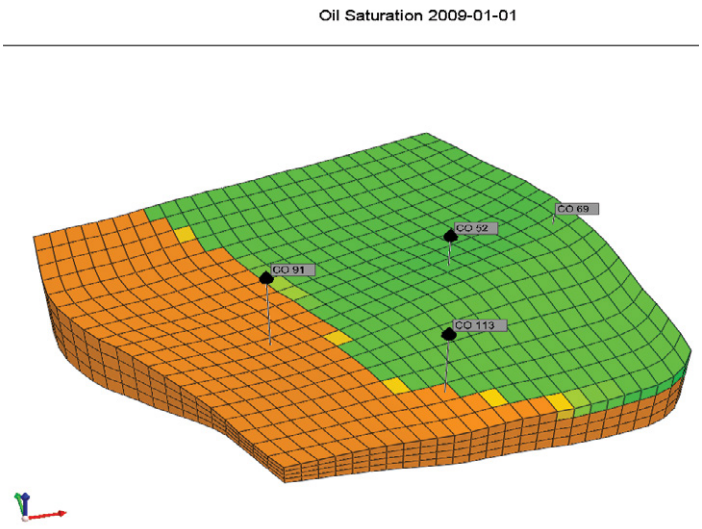

Figure 15: 3D view of oil saturation at 2009 and 2019 without water-flood.

result have the same environment of deposition (Figures 2, 3 and Appendix 1, Figures 19, 20). The composite type log of CO-30 sand which is highlighted in red rectangular dimension (Appendix 1, Figure 18) was used as a guide since it is the most profound

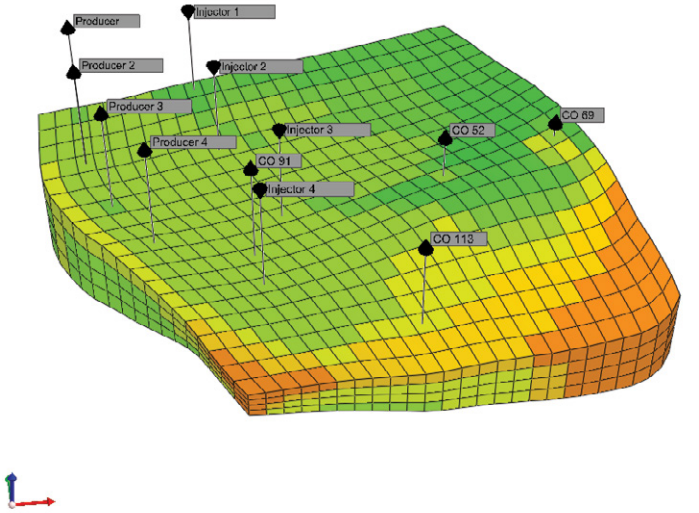

Figure 16: 3D view of oil saturation at 2019 after water-flood.

sand package of southwest Catshill field and also the central focus of the study. Well logs of wells within the selected area of study were correlated using the type log as reference point. The depth measure used in the correlation was the standard true vertical depth (Appendix 1, Table 13). The correlation included structural correlation for each faulted block to investigate the displacement of the CO-30 sand package with respect to the fault movement (Figure 3). Sand in communication or not and either sealing or non-sealing were identified (Appendix 1, Table 9). The faults identified were mostly normal faults (Figures 2, 3 and Appendix 1, and Figures 19, 20).

Building the structure map

By utilizing information gathered on oil water contact, depth and faults (Appendix 1, Table 10 and 13) the structure map for the study area was generated using Petrel Software (Figure 4). The true vertical depths (TVD) for each well was calculated from the measured depth (MD) of the well logs. These values were subtracted from the elevation (Rotary Table or Kelly Bushing) (Appendix 1, Table 13). These top and bottom values were placed on the structure map at the specific location of the respective wells taking the regional faulting of the area into account. The map was then contoured using Petrel. This was done by also taking into consideration the existing faults and the additional faults based on contour misties and fluid anomalies. Due to the poor quality of the available seismic data, the use of the dipmeter logs were used to verify the direction in which the structure dips and orients. The depth range derived from the map is from 1500ft to 2500ft TVD (Appendix 1, Table 12). The faults were used to label the blocks in the field Block as A, B, C, and D (Figure 4 and Appendix 1, Table 11).

Construction of net sand map

To get the total net sand, the maximum and minimum shale line was drawn for the SP and a 50% line was drawn between the maximum and minimum line as the cut off value for shales and sands (Figure 5). To the right of the 50% line is considered to be shale while to the left of the line is sand (Figure 5). The Interval

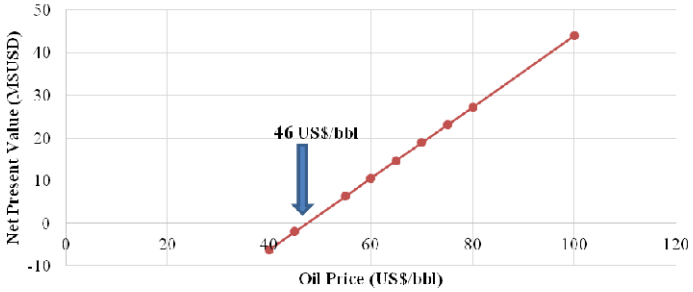

Figure 17: NPV variation with oil price.

Table 1: Rock and fluid properties analyzed for fault block C.

													Indonesian			Simandaux		
Wells #	SP Shale	SP Clean	SP Log	Vshale	Rt	Ro	Rmf (Ohm)	Measured Temperature (°F)	Formation Temperature (°F)	BHT (°F)	R_{mf} @ formation temperature	RW (Silver Bassiouni method)	Porosity	AS	BS	SW	AS	BS	SW
CO 91	0	-45	-36	20	12	2	0.9	85	113.6	115	0.7	0.22	0.31	2.45	0.58	0.331	0.019	0.19	0.42
CO 13	0	-45	-35	22	8	2	1	85	118.6	120	0.7	0.24	0.31	2.02	0.53	0.392	0.034	0.31	0.52
CO 113	0	-50	-30	40	15	2.4	3.2	80	108.7	110	2.4	0.27	0.31	2.5	1.2	0.27	0.037	0.19	0.4
CO 20	0	-50	-30	40	18	2	0.1	84	118.2	120	0.1	0.05	0.31	3	1.44	0.225	0.006	0.03	0.17
CO 123	0	-30	-20	33	20	4	2.2	82	101.7	103	1.8	0.12	0.31	2.24	0.89	0.32	0.01	0.06	0.24
CO 52	0	-83	-60	28	8	1.8	1.1	99	119.7	121	0.9	0.13	0.31	2.11	0.7	0.356	0.023	0.17	0.39
CO 75	0	-24	-20	17	16	1.8	0.7	90	116.6	118	0.5	0.26	0.31	2.98	0.59	0.28	0.014	0.17	0.4
Average total				29					113.9	115.3		0.18	0.31			0.311			0.36

Table 2: Total fluids in place in fault bock C from CMG.

Item	Fluid Production		
	Oil (MSTB)	Gas (MMSCF)	Water (MSTB)
Cumulative Production	7490.1	3630.4	0.29402
Current fluids in place	20046	457.74	7101.4
Production Rates	0.02989	5.68E-04	1.85E-06
Average reservoir pressure excluding water zone	51.81psia		

Table 3: Cumulative production from the field (Fault Block C) after 10 years by primary depletion.

Item	Fluid Production		
	Oil (MSTB)	Gas (MMSCF)	Water (MSTB)
Cumulative Production	7490.1	3630.4	0.29402
Current fluids in place	20046	457.74	7101.4
Production Rates	0.02989	5.68E-04	1.85E-06
Average reservoir pressure excluding water zone	51.81psia		

Table 4: Production response from staggered line drive pattern from beginning of production.

Injection rate (b/d)	Cumulative Oil Produced (MSTB)	Cumulative gas Produced (MMSCF)	Cumulative water Produced (MSTB)	Cumulative water injected (MSTB)	Average reservoir pressure excluding water zone (psia)	Recovery Factor (%)
1000	13258	3803.9	90981	98205	49.45	48.14
1500	12718	3730.1	137708	147186	72.33	46.18
2000	12827	3663.5	183863	195002	96	46.57
2500	13151	3606.7	216860	228692	112.89	47.75
3000	13177	3597.8	222338	234265	115.9	47.84
3500	13177	3597.8	222338	234265	115.9	47.84
4000	13177	3597.8	222338	234265	115.9	47.84
4500	13177	3597.8	222338	234265	115.9	47.84
5000	13177	3597.8	222338	234265	115.9	47.84

Table 4: Production response from staggered line drive pattern from beginning of production.

Well Name	Field Cumulative oil production up to 2009 (bbl)	Cumulative oil Production @1000b/d up to 2009	Cumulative oil Production (bbl) from waterflood @1000b/d up to 2019
CO 52	4454	675497	675497
CO 69	59900	579857	579857
CO 91	254618	802192	858233
CO 113	5937	1290000	1330000

Table 5: Comparison of recorded field cumulative oil production history with waterflood oil production.

Well Name	Field Cumulative oil production up to 2009 (bbl)	Cumulative oil Production @1000b/d up to 2009	Cumulative oil Production (bbl) from waterflood @1000b/d up to 2019
CO 52	4454	675497	675497
CO 69	59900	579857	579857
CO 91	254618	802192	858233
CO 113	5937	1290000	1330000

Table 6: Injection from beginning of production using five spot pattern.

Injection rate (b/d)	Cumulative Oil Produced (MSTB)	Cumulative gas Produced (MMSCF)	Cumulative water Produced (MSTB)	Cumulative water injected (MSTB)	Average reservoir pressure excluding water zone (psia)	Recovery Factor (%)
1000	12756	3644.9	88013	97941	93.74	46.32
1500	13182	3510.7	128993	140752	134.36	47.86
2000	13628	3406.2	155445	167646	161.42	49.48
2500	13729	3381.6	161705	174020	168.37	49.85
3000	13729	3381.6	161705	174020	168.37	49.85
3500	13729	3381.6	161705	174020	168.37	49.85
4000	13729	3381.6	161705	174020	168.37	49.85
4500	13729	3381.6	161705	174020	168.37	49.85
5000	13729	3381.6	161705	174020	168.37	49.85

that is identified during the correlation that contains both sand and shale is known as the Net Gross Interval. The amount of shale that exists in the interval is then determined and is subtracted from the Net Gross Interval to yield the Total Net sand that was deposited in the system. These thicknesses values were then used for mapping the net sand map and contoured again using Petrel Software (Figure 6).

Generating net oil sand (NOS) map

The Net Oil Sand Map shows the distribution of the hydrocarbons within the net sand in relation to the faults which form traps in the Catshill Field. The structure map and well log data were used to calculate the total net oil sand thickness. The NOS map took into consideration contacts (GWC/OWC) which showed the transitioning from hydrocarbon to water. For the generation of the NOS map (Figure 7), only resistivity curves were available therefore a cut off resistivity value of 4 ohms was used to determine whether hydrocarbon exists or not (Figure 5). A value of 4 ohms was used since this value is typically used for the identification of hydrocarbons in the onshore southern basin Trinidad. The map was then generated using Petrel Software.

Formation evaluation

Volume of shale estimation: Utilizing the spontaneous Potential log, the shale baseline and clean sand line were drawn for each well log within Fault block C and VShale for respective zones of interest were estimated (Table 1). Equation [1] was used to compute for the volume of shale for each well using their well logs.

$$V_{sh} = \frac{SP_{sh} - SP}{SP_{sh} - SP_{cl}}$$ Equation (1)

Where,

SP_{SH}-SP value at shale baseline

SP-SP in the zone of interest (read from the log)

SP_{cl} Maximum Sp deflection from the clean wet zone [26].

Water Resistivity (Rw)

The water resistivity for the zones was determined using Silver and Bassiouni method [27] and the Spontaneous Potential Log data. Using the Silver and Bassiouni method (Appendix 1, Figure 21), the resistivity of water for the various wells in the Fault block C was determined same as illustrated by well CO-20 in Appendix 1, Figure 21. The formation temperature was first estimated in Equation 3. The Rmf was converted to formation temperature. This was done using Arp's equation as show below [28].

$$R1 + (T1 + 7) = R2 (T2 + 7)$$ **Equation (2)**

The Formation temperature (T_f) was estimated using the following formula:

Table 7: Water flooding from 2009-2019 and recovery factor.

Injection rate (b/d)	Cumulative Oil Produced (MSTB)	Cumulative gas Produced (MMSCF)	Cumulative water Produced (MSTB)	Cumulative water injected (MSTB)	Average reservoir pressure excluding water zone (psia)	Recovery Factor (%)
1000	10653	3753.1	9020.6	16072	68.09	38.68
1500	10728	3762	15022	24108	92.71	38.95
2000	10766	3745.9	21824	32144	139.78	39.09
2500	10795	3742.3	29255	40180	194.81	39.2
3000	10825	3739.8	37049	48216	240.8	39.31
3500	10854	3738.7	44944	56252	287.72	39.41
4000	10876	3737.4	52863	64288	334.85	39.49
4500	10896	3736.5	60803	72324	382.21	39.56
5000	10913	3736	68761	80360	429.71	39.62

Table 8: Water injection rates and cumulative fluid production from 2009-2019.

Injection rate (b/d)	Cumulative Oil Produced (MSTB)	Cumulative gas Produced (MMSCF)	Cumulative water Produced (MSTB)	Cumulative water injected (MSTB)	Average reservoir pressure excluding water zone (psia)	Recovery Factor (%)
1000	10038	3719.7	6501.8	16072	168.69	36.45
1500	10081	3718.4	13566	24108	332.06	36.6
2000	10120	3718.3	21423	32144	407.37	36.75
2500	10158	3718.7	29319	40180	491.12	36.88
3000	10192	3718.7	37233	40216	578.47	37
3500	10217	3718.5	45160	56252	666.78	37.09
4000	10239	3718.3	53075	64268	758.16	37.18
4500	10256	3718.1	60990	72324	854.76	37.24
5000	10269	3717.7	68920	80360	943.94	37.29

$$T_f = T_s + D_f \frac{BHT - T_s}{TD}$$ **Equation (3)**

Determination of water saturation

The sand in the fault block is a shaly sand and therefore in the estimation of water saturation, Simandoux and Indonesian equations were used. Based on water resistivity values calculated, a criterion of Rw<0.2 for use of Simandauex equation given by equation [5,29] and Rw>0.2 for use of Indonesia equation thus Equation 4 were applied to determine the water saturation Table 1.

$$\frac{1}{\sqrt{R_t}} = \left(\frac{V_{sh}\left(1 - v_{sh/2}\right)}{\sqrt{R_{sh}}} + \frac{\phi^{\frac{m}{2}}}{\sqrt{aR_w}} \right) S_{we}^{\,n/2}$$ **Equation (4)**

The simaneoux equation can be written as

$$Sw = -As + \sqrt{\left(As^2 + Bs\right)}$$

Where : $$As = \frac{Rw * Vsh}{\phi^2 * 2 * Rsh}$$

And $$Bs = \frac{Rw}{\phi^2 * Rt}$$ **Equation (5)**

Waterflood Simulation

Information gathered from the geological analysis and formation evaluation of the fault block (Table 1, Appendix 1, Tables 10, 11, 12 and 13) were used to simulate waterflooding by paying key attention to the geological behaviour of the field as outlined above.

Water injection above the bubble point pressure (development plan 1)

The structure map, net sand map and net oil sand map were exported from petrel to CMG for the detailed simulation. According to the field reports reviewed, the field is a matured field and has been produced from 1950 to 2009. To inject water above the bubble point pressure, the field was treated as a new field. In this case, the field production history was ignored. Then efficacious and judicious selection of waterflooding pattern was done by utilizing both five spot pattern and staggered line drive. Here, water was injected from the beginning of production (1950). With the five spot pattern (Figure 13), four injection wells and one producer located in the center of the reservoir was used. The injectors and producers were placed based on the distribution of the oil saturation and the geology of the field was used (Figure 15 and 16). The staggered line drive consisted of five producers and four injectors (Figure 10). All the four (4) layers were perforated for the production wells but only the 4th layer was perforated for the injection wells. The rational was to inject water from beneath to move to surface by gravity to sweep enough oil to the surface. Pressure was set at initial reservoir pressure of 2450psia. The field was produced from 1951 to 2009. That was the start of production to the end of last production history of the field. This was done to know the recovery if the field was produced with

waterflooding from the beginning when reservoir had enough energy. The simulation period was extended for additional 10 years to compare production response (from 1951-2019). These had long span which practice will be highly dependent on economics. This methodological processes was carried out to determine if it is appropriate to introduce waterflooding at the beginning of production when pressure is high above the bubble point pressure.

Water injection below the bubble point pressure (development plan 2) for brownfields

The matured field data was used to build the model and waterflooded for 10 years to see the production response. The field is matured and undersaturated with pressure below the bubble point. After building the static and dynamic reservoir model and doing prediction run to see the field production by primary drive mechanism (Figure 9), water was injected from end of production data to the next ten years (2009-2019) to ascertain the production response. This was also done by utilizing both five spot pattern (Table 8) and staggered line drive (Table 7) of the same well arrangement as in water injection above the bubble point. This provided good basis for comparison. But here, because of the existing wells on the field, some of these wells were converted to injectors due to high water oil ratio (WOR of 5:1) was deemed uneconomic [9] to produce and was converted to injectors. Also, based on the distribution of the oil saturation and existing well arrangements, new injection and production wells were also placed to increase sweep efficiency. Here, water injection rate was varied from 1000b/d to 5000b/d to get injection rate with better recovery, low water cut and economic (Tables 7 and 8). The reservoir pressure and other petrophysical properties that were utilized are in Appendix 1, Table 12. The well arrangements were the same as in injection above the bubble point to provide good bases for comparison.

RESULTS

Formation evaluation and analysis for block C

Table 1 shows the calculated rock and fluid properties for the fault block. These properties were used extensively in the overall field development processes. The well logs used were analyzed to evaluate reservoir properties such as shale volume, water saturation, sand thickness and permeability in order to obtain the hydrocarbon potential of the wells.

History matching to validate reservoir model built

After the geological information and the reservoir rock and fluid properties has been fed into the CMG launcher to build the reservoir model, a history match was performed. There was an observed close match for all the wells in fault block C enough to validate the model (Figure 8). Some wells did not match exactly due to the quality of the data. However, the level of deviation does not present significant difference to affect quality. From the Figure 8, the maximum production per day was 180b/d which decreased upon further production with respect to decline in pressure and time increase.

Fault block c prediction run

After the model has been validated by history matching, the capability of the fault block C to produce for a period of ten (10) years under primary energy drive (solution gas drive) was assessed. The field was produced for 10 years (from 2009-2019) and a decrease in trend of production was observed (Figure 9). The cumulative production was 7490.1 MSTB of oil of the total oil in place (27.541MMSTB) representing a recovery factor of 27.2% (Table 2 and 3).

Injection from beginning of production and above the bubble point pressure utilizing staggered line drive pattern

Simulation was done to determine how oil could have been recovered if water injection was initiated at the beginning of the production period. There was high oil recovery factor with low water injection rate (Table 4). There was high oil production from the staggered line drive pattern at an injection rate of 1000b/d with recovery factor of 48.14% (Table 4). The irreducible oil saturation occurred at injection rate of 2500b/d (Table 4). A comparison of already field production records with when waterflood was done from the start (1951) was done and this is presented in Table 5.

Figure 10 shows the location of injectors and producers for the staggered line drive pattern for fault block C of the Catshill field in aerial view. Most of the oil was saturated in the third (3rd) and fourth (4th) layers of the block. In this regard, the new injectors and producers were located around this area (That is, the thickest zone). Also, the cumulative oil produced with and without waterflooding showed that waterflooding produced much higher production (Figures 11, 12).

Utilizing five spot pattern for injection from beginning of production

Figure 13 shows the 3D view of the location of the injectors and producers in the five spot pattern arrangement for production from above bubble point.

Similarly, if waterflood was done at start of production, a much higher recover factor of 49.85% at 2500b/d would have being recovered as against the 27.2% recorded from primary recovery. Although the staggered line drive produced 48.34% at low injection rate of 1000b/d. Irreducible oil saturation was reached at 2500b/d same as in staggered line drive (Table 6).

Water injection below the bubble point pressure using staggered line drive

Table 6 show that at injection rate of 3500b/d, a much higher recovery was recorded (39.41%) which was comparatively higher than utilizing five spot injection pattern (Table 6).

Injecting below the bubble point using five spot pattern

In order to get best pattern to yield better sweep efficiency, five spot pattern was applied to the model below the bubble point. The staggered line drive gave higher recovery factor compared to the five spot pattern arrangement below the bubble point (Tables 7 and 8). Figure 14 shows a close match in oil recovery by injecting at same injection rates for 10 years but with higher recoveries from

staggered line drive making it a better option. The oil saturation without waterflood (production by primary energy) shows very little differences for the 10-year prediction (Figure 15). The effect of water injection at 3500b/d for the 10-year period (from 2009-2019) as shown in Figure 16.

Figure 17 illustrates changes in NPV as the oil price varies. As the oil price increases, the NPV also increases. The project will not be profitable if the oil price goes below 46 $/bbl. This could imply profitability at comparatively low prices.

DISCUSSION

The geology of the area of study was carefully analysed [30,31]. This followed formation evaluations to obtain accurate rock and fluid properties necessary to determine the oil in place and remaining oil that can be exploited (4,19,20,31-33]. The Oil in Place is accurately obtained by the best estimate of rock and fluid properties such as water saturation, shale volume, porosity and permeability (Table 1 and Appendix 1, Table 12) but often comes with uncertainties collaborating with findings [33]. The porosity of the field was determined from core sample analysis as 0.31 (Appendix 1, Table 12) which represents a good value [34]. The permeability ranged from 137mD to 618mD with oil and gas having an API° gravity between 35 to 40 (Appendix 1, Table 12). The permeability range was necessary to allow to movement of fluids which is equally reported [30,35,36] that adequate permeability is required to permit movement of fluids at an acceptable rate with available well spacing. The API gravity (Appendix 1, Table 12) presents a good case of light oil and suitable for waterflooding.

Waterflooding has been predominantly used to recover oil from most reservoirs worldwide [37]. Therefore, the possibility was assessed in the field development for plan (1) injection above the bubble point and plan (2) injection below the bubble point. After estimating the amount of oil that can be recovered by solution gas drive, there was the need to implement the waterflooding since the recovery was low (27.2%) which agrees to findings [31,38] that the lifecycle for primary recovery is generally short and the recovery factor is usually low. Waterflooding is less expensive and can recover considerable amount of oil with better sweep efficiency [39-42]. The Static reservoir model built was history matched to the field production history to validate the model (Figure 8). Some of the reservoir properties were altered within the range of values determined (Table 1 and Appendix 1, Table 12). For instance, the permeability for the various layers was varied between 137 mD and 618 mD as well as varying the thickness. The constraints were set based on the properties of the reservoir. For instance, the bottom hole pressure was set at 2450 psia and the surface oil flowing rate set 'Altered' to take into account the varying oil flow rate of the field at particular pressure of the field [31]. The amount of oil recovered over the ten-year period was less than half of the total oil in place [31].

The Waterflooding was carried out first from the beginning of the initiation of the field when pressure was high to determine how much could have been produced if the waterflood was started from the beginning when the field was first been developed. It was observed that the recovery factor was the highest (about 49.85% with low water injection rates) (Tables 4 and 6). Although some researchers reported that on the average, the recovery factor for oil is about 35% [12-14]. The recorded value could be due to the availability of enough energy [43] and the well arrangement pattern in the reservoir therefore small water injection rates can result in good recovery with corresponding low water cut and WOR [42,44,45] This underscores with a similar study where the macroscopic sweep efficiency was maximized by controlling the injection and production rates [46]. The production from the waterflood was compared with existing production history and the waterflooded reservoir recorded much higher cumulative oil production (Table 5). This implies that if waterflooding was implemented right at the start of the field development, much oil would have been recovered (Tables 4 and 6). According to Sallam et al. [47] the implementation of waterflood increased oil production by 31% of the original oil in place.

With respect to field development plan two, the best well arrangement pattern was the staggered line drive (Table 7 and Figure 14). This arrangement yielded a recovery factor of 39.41% at injection rate of 3500b/d which compares with findings that on average Recovery Factor from mature oilfields around the world is between 20% and 40% [48] With optimized waterflooding, there is potential to increase the amount of petroleum that can be economically produced from matured reservoirs [15]. Comparatively, the recovery was low for the matured field than production above the bubble point. This was attributed to the low reservoir pressure [42]. At this injection period the pressure had fallen below the bubble point pressure and therefore would not have enough reservoir energy to recover much oil over the ten-year period compared to when pressure was above the bubble point [42,49] It is important to note that, in order to achieve good recovery from the Fault Block C, additional four injectors and four producers were placed in the reservoir (Figure 16). This accounted for the additional oil production which is expected to be obtained following the field development plan implementation. This is in agreement that waterflooding improve oil production rate [50,51]. Considering the amount of oil recovered, it means that some of the oil still remained trapped in the ground [52]. According to Meshioye et al. [25] on the average, waterflood can recover about one-third of the original oil in place (OOIP), leaving behind about two-thirds as observed in this situation. At some point of the injection rate, the water cut increased and oil production decreased (Table 4). This could be due to water breakthrough and water outrunning the oil and therefore producing at a much faster rate than the oil production rate [53].

It must be emphasized that with the increase of the injected water volumetric flow rate there is a consequent increase in the water produced, which it is a negative aspect of the water injection method (Tables 4, 6, 7 and 8). The recovery factors were an indication that implementing waterflood in the development of the Fault Block C would be paramount. According to Strandli [54] there is a strong relationship between IOR investments and economics (Appendix 1, Table 14). As such, the profitability and suitability of the project was evaluated under various price fluctuations taking into account NPV variation with respect to oil price per US$/bbl. during the life of the project by running a sensitivity analysis. A project profitability indicator requires NPV and P/I ratio to be more than zero. This project had favorable P/I ratio (1.04%) implying that the risk of undertaking the project is not a critical factor (Table 14). At low prices of less than or equal to 45 US$/bbl., negative NPV is seen (Figure 17) translating that at these prices investment costs exceed

return on revenue and will render project not ideal (abandon). This outcome is no different from the report of Layti in 2017 [55] that the simultaneous increase in investment costs could result in negative NPV enhancing the chance of unprofitable project. This negative NPV scenario (Figure 17) could be possible with waterflooding of matured field due to extra expenditure on water treatment facilities, installation costs, injector and producer wells and also drilling for reliable water source. However, the waterflood project for the field development could stand some varying prices (46$/bbl-100 US$/bbl) having positive NPV (Figure 17) and still be profitable except for prices below 46 US$/bbl (Figure 17) which is similarly reported by Strandli [54].

CONCLUSION

Based on the results of the study, the following significant deductions can be made

1. When water was injected above the bubble point pressure, high recovery factor was seen. This concludes that when water is injected at the beginning of field development when pressure is high enough can lead to high oil recovery
2. Using waterflood for brown field development can recover some amount of oil as proven by this study but associated with increased CAPEX and operating and cannot stand very low prices
3. From the economic analysis of the field development plan, the implementation of the project taking into account Productivity index, NPV, DCFROR and payout time is recommendable but will depend highly on company's financial ability and decision.

RECOMMENDATIONS

Deducing from the study, the following recommendations can be given for further research and development of oil fields:

1. When developing new field with waterflooding it will be advantageous to initiate waterflooding from the start since it yields higher oil recovery.
2. The use of other Enhanced Oil Recovery (EOR) method should be studied and tested for further development of matured fields although water injection proved laudable but the recovery was not so high.
3. Since the fault blocks identified are not in communication, it is paramount to undertake further detailed and technical studies in assessing the feasibility of developing the other Fault Blocks especially Fault Block D of the CO-30 sand of the Catshill field because of the reasonable by-passed hydrocarbon accumulation in such block.

REFERENCES

1. Mezzomo CC, Schiozer DJ. Field development planning optimization using reservoir simulation. Universidade Estadual de Campinas. 2019;2:1-8.
2. Alqahtani MH. A systematic approach to offshore fields development using an integrated workflow. Master's Thesis, Texas A&M University, US in 2010.
3. Blaskovich FT. Historical problems with old field rejuvenation. Presented at the SPE Asia Pacific Conference on Integrated Modelling for Asset Management, Society of Petroleum Engineers, Yokohama, Japan in 2000.
4. Babadagli T. Development of mature oil fields—A review. J Pet Sci Eng. 2007;57:221-246.
5. Sinanan B, Evans D, Budri M. Conceptualizing an improved oil recovery master plan for Trinidad and Tobago. Paper Society of Petroleum Engineers 180853 presented at the Society of Petroleum Engineers Trinidad and Tobago Section Energy Resources Conference. Port of Spain, Trinidad and Tobago in 2016.
6. Ernst and Young. Enhanced oil recovery methods in Russia: Time is Off the Essence, UK in 2013.
7. Ministry of Energy and Energy Industries. The Petroleum Taxes Act. 2009;75:04
8. Koldewijn BW. Sand Distribution in the "Cruise" and "Forest" Sediments of Ortoire. *Geological Report 1145 (unpublished)*. Shell Trinidad Ltd in 1961.
9. Archie C. Geological Evaluation of the Catshill Sands in the Catshill Field. Report by the Petroleum Company of Trinidad and Tobago. 1989:3-8.
10. CERA. Finding the Critical Numbers: What Are the Real Decline Rates for Global Oil Production? Private report written by Peter M. Jackson and Keith M. Eastwood in 2007.
11. ExxonMobil. A report on energy trends, greenhouse gas emissions, and alternative energy, information to shareholders: February 2004
12. Gaffney-cline and Associates. Mature Fields Optimisation. Alton, Hampshire GU34 4PU, United Kingdom. Accessed May 23, 2019.
13. Höök M, Hirsch R, Aleklett K. Giant oil field decline rates and their influence on world oil production. Energy Policy. 2009;37:2262–2272.
14. Litvak M, Gane B, McMurray L, Skinner R . Field development optimization in a giant oil field in Azerbaijan and a mature oil field in the North Sea. Presented at the offshore technology conference, Offshore Technology Conference, Texas, USA in 2007.
15. Udy J, Hansen B, Maddux S, Petersen D, Heilner S, Stevens K. Review of field development optimization of waterflooding, EOR, and well placement focusing on history matching and optimization algorithms. Processes. 2017;5:-25.
16. Ahmed T. Reservoir Engineering Handbook. Gulf Professional Publishing. Burlington. Massachusetts, US in 2006.
17. Craft BC, Hawkins MF, Terry RE. Applied petroleum reservoir engineering. Prentice-Hall Englewood Cliffs, 3rd edition in 1959, Upper Saddle River. New Jersey, USA.
18. Dake LP. Fundamentals of reservoir engineering. Elsevier, Amsterdam, The Netherlands in 1983.
19. Wang P, Aziz K, Litvak ML. Optimization of Production from Mature Fields. Presented at the 17th World Petroleum Congress, World Petroleum Congress, Rio de Janeiro, Brazil. 2002:1-5.
20. Wen-Rui H. Necessity and feasibility of PetroChina: Mature Field Redevelopment. Petroleum Exploration and Development. 2008;35(1):1-2.
21. Fanchi JR. Principles of applied reservoir simulation. Gulf Professional Publishing in 2005.
22. Aziz K, Settari, A. Petroleum reservoir simulation. Chapman and Hall in 1979, Norwell Massachusett, US.
23. Cancelliere M, Viberti D, Verga F. A step forward to closing the loop between static and dynamic reservoir modeling. Oil and Gas Science and Technology in 2014.

24. Seiler A, Rivenaes JC, Aanonsen SI, Evensen G. Structural Uncertainty Series. Society of Petroleum Engineers in 2009 at Richardson, Texas, US.

25. Meshioye O, Mackay E, Chukuwezi M. Optimization of waterflooding using smart well technology. Paper Society of Petroleum Engineers 136996 presented at the 34th annual SPE international conference and exhibition held in 2010 at Tinapa, Calabar, Nigeria.

26. Abiodun Matthew A. Passive or Spontaneous Logs. Lecture notes. 2014:31.

27. Silva P, Bassiouni Z. A Shaly Sand Conductivity Model Based on Variable Equivalent Counter-ion Conductivity and Dual Water Concepts. SPWLA Transaction paper RR in 1985.

28. David Schechter. Formation evaluation PETE 663, Passive measurements-sp in 2010.

29. Simandoux P. Dielectric measurements on porous media: application to measurement of water saturation: Study of the behavior of argillacious formation. SPWLA, Houston. 1963:97-124.

30. Willhite FP. Waterflooding, Textbook Series. Society of Petroleum Engineers, Dallas, USA. 1986:3.

31. Zitha P, Felder R, Zornes D, Brown K, Mohanty K. Increasing hydrocarbon recovery factors. Society of Petroleum Engineers in 2019.

32. Egwebe O. Petroleum exploration in the Niger Delta. NAPE Publication. 2003;3:3-10.

33. Ayoola EO. Volumetrices of field in Eastern Niger Delta, Proceedings of the 23rd Annual Nape International Conference, Lagos Nigeria. 2004:10-16.

34. Tissot BP, Welte DH. Petroleum formation and Occurrence. Springer-Verlag, Berlin. 1984:356-361.

35. Craig FF. The Reservoir Engineering Aspects of Waterflooding. Society of Petroleum Engineers in 1971, New York, Dallas, USA.

36. Rose SC, Buckwalter JF, Woodhall RJ. The Design of Engineering Aspects of Water-flooding. Society of Petroleum Engineers in 1989, Richardson in Texas, USA.

37. Craft BC, Hawkins MF. Applied Petroleum Reservoir Engineering. Prentice Hall PTR. Englewood Cliffs in 1991, New Jersey, US.

38. Terry RE. Enhanced Oil Recovery. In Encyclopedia of Physical Science and Tchnology, 3rd Edition, Robert A. Meyers Ed., Academic Press, 2001;18:503-518.

39. Morsy S, Shengand JJ, Ezewu RO. Potential of Waterflooding in Shale Formations. Paper Society of Petroleum Engineers 167510, presented at the Society of Petroleum Engineers Nigeria Annual International Conference and Exhibition, Lagos, Nigeria in 2013.

40. Asheim H. Optimal Control of Water Drive. Society of Petroleum Engineers.15978-MS General in 1987.

41. Adeniyi OD, Nwalor JU, Ako CT. A review on water-flooding problems in Nigeria's Crude Oil Production. J Disper Sci Technol. 2008;29(3):362-365.

42. Muggeridge A, Cockin A, Webb K, Frampton H, Collins I, Moulds T, et al. Recovery rates, enhanced oil recovery and technological limits. Philos Trans A Math Phys Eng Sci. 2014;13:372.

43. Correie B, Silva G, Cunha A, Santos B. Water Injection for Oil Recovery by using Reservoir Simulation via CFD. Int J Multiphys. 2017;11(1):83-90.

44. Bondino I, Nguyen R, Hamon G, Ormehaug PA, Skauge A, Jouenne S. Tertiary polymer flooding in extra-heavy oil: an investigation using 1D and 2D experiments, core scale simulation and pore scale network models. International Symposium of the Society of Core Analysts, Austin, Texas, USA in 2011.

45. Stephen CM, Duane BD, Richard NM. Waterflood Optimization of the Buffalo Coulee Bakken Heavy Oil Pool of Southwestern Saskatchewan, Society of PetroleumEngineers, SPE30285 in 1995.

46. Asadollahi, M., Nævda, G. l. and Shafieirad, A. Efficient workflow for optimizing well controls. J Petrol Sci Eng. 2012;82-83:66-74.

47. Sallam S, Nasr M, Ahmad MM. The Effect of Water Injection on Oil Well Productivity. Conference Paper in 2015.

48. Sandrea I, Sandrea R. Recovery factors leave vast target for EOR technologies. Oil Gas J. 2007;105:44–47.

49. Wang FP, Ambrose WA, Hentz TF. Engineering and Characterization of Giant East Texas Oil Field: North and South Pilot Studies. Proc., Society of Petroleum Engineers the Annual Technology Conference and Exhibition. Denver. Colorado. USA in 2008.

50. Morrow N, Buckley J. Improved Oil Recovery by Low-Salinity Waterflooding. Journal of Petroleum Technology. 2011;63(5):106-112.

51. Khatib S, Walsh JM. Extending the Life of Mature Assets: How integrating subsurface and surface knowledge and best practices can increase production and maintain integrity. Society of Petroleum Engineers-170804-MS Annual Technical Conference and Exhibition held in Amsterdam, The Netherlands. 2014;6-8

52. Society of Petroleum Engineers. Microscopic Efficiency of Waterflooding in 2014.

53. Van Essen G, Zandvliet MP, Van DH, Bosgra O, Jansen J. Robust optimization of oil reservoir flooding. In Proceedings of the IEEE International Conference on Control Applications in 2006.

54. Strandli A. Rystad Energy venter ytterligere aktivitetsfall offshore. Hegnar in 2017 Retrieved from http://www.hegnar.no/Nyheter/Energi/2017/03/Rystad-Energy-venter-ytterligere-aktivitetsfall-offshore.

55. Layti F. Profitability of Enhanced Oil Recovery. Economic Potential of LoSal EOR at the Clair Ridge Field, UK. Master's Thesis, University of Stavanger, Norway in 2017.